CrossMark
click for updates

View Article Online
View Journal

RSC Advances

This article can be cited before page numbers have been issued, to do this please use: M. Ravikanth and S. Kumar, *RSC Adv.*, 2014, DOI: 10.1039/C4RA10807H.

This is an *Accepted Manuscript*, which has been through the Royal Society of Chemistry peer review process and has been accepted for publication.

Accepted Manuscripts are published online shortly after acceptance, before technical editing, formatting and proof reading. Using this free service, authors can make their results available to the community, in citable form, before we publish the edited article. This *Accepted Manuscript* will be replaced by the edited, formatted and paginated article as soon as this is available.

You can find more information about *Accepted Manuscripts* in the Information for Authors.

Please note that technical editing may introduce minor changes to the text and/or graphics, which may alter content. The journal's standard Terms & Conditions and the Ethical guidelines still apply. In no event shall the Royal Society of Chemistry be held responsible for any errors or omissions in this *Accepted Manuscript* or any consequences arising from the use of any information it contains.

ROYAL SOCIETY OF CHEMISTRY

www.rsc.org/advances

View Article Online
DOI: 10.1039/C4RA10807H

Published on 19 November 2014. Downloaded by University of Chicago on 19/11/2014 19:01:19.

Graphical Abstract

2-Formyl Boron-Dipyrromethene as Key Synthon to Prepare Functionalized *Meso*-Boron Dipyrromethenyl Porphyrin Building Blocks

Sunit Kumar and Mangalampalli Ravikanth*

Indian Institute of Technology, Powai, Mumbai, 400076 India. Fax: 91-22-5723480

Tel: 91-22-5767176; E-mail: ravikanth@chem.iitb.ac.in

A series of functionalized *meso*-BODIPYnyl porphyrin building blocks were synthesized using 2-formyl BODIPY as key precursor.

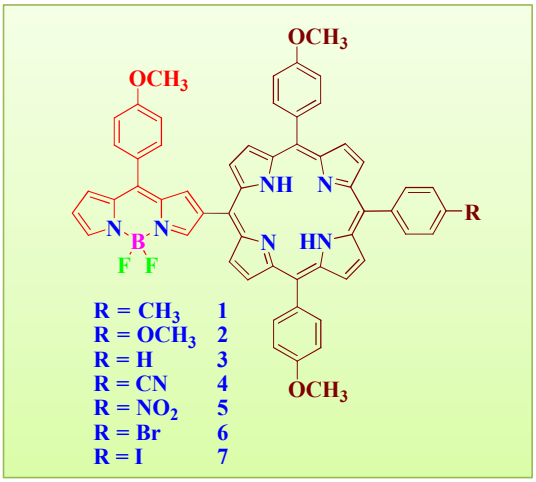

RSC Advances Accepted Manuscript

View Article Online
DOI: 10.1039/C4RA10807H

Published on 19 November 2014. Downloaded by University of Chicago on 19/11/2014 19:01:19.

2-Formyl Boron-Dipyrromethene as Key Synthon to Prepare Functionalized *Meso*-Boron Dipyrromethenyl Porphyrin Building Blocks

Sunit Kumar and Mangalampalli Ravikanth*

Indian Institute of Technology, Powai, Mumbai, 400076 India. Fax: 91-22-5723480

Tel: 91-22-5767176; E-mail: ravikanth@chem.iitb.ac.in

Abstract

A series of functionalized *meso*-boron dipyrromethenyl porphyrin building blocks were synthesized by condensing one equivalent of readily available 2-formyl boron dipyrromethene (2-formyl BODIPY) with two equivalents of *meso*-anisyl dipyrromethane and one equivalent of functionalized aldehyde under mild acid catalyzed conditions followed by column chromatographic purification and afforded in 5-7% yields. The *meso*-BODIPYnyl porphyrins are freely soluble in common organic solvents and characterized by mass, spectral and electrochemical techniques. The presence of BODIPY unit directly at the *meso*-position alters the π-delocalization of the porphyrin macrocycle. The compounds are weakly fluorescent because of effective charge transfer between porphyrin and BODIPY units leading to the formation of low lying charge transfer state. The *meso*-BODIPYnyl porphyrin-BF_2-smaragdyrin conjugate was synthesized by coupling *meso*-BODIPYnyl porphyrin building block containing *meso*-iodophenyl group with ethynyl BF_2-smaragdyrin under Pd(0) coupling conditions. The spectral and electrochemical studies indicated that the photo-induced electron transfer is the predominant process in *meso*-BODIPYnyl porphyrin-BF_2-smaragdyrin conjugate.

Key words: Boron-dipyrromethene, porphyrin, functionalization, smaragdyrin, electrochemistry.

RSC Advances Accepted Manuscript

View Article Online
DOI: 10.1039/C4RA10807H

Published on 19 November 2014. Downloaded by University of Chicago on 19/11/2014 19:01:19.

Introduction

Boron difluoride dipyrrin complexes (BODIPY) are very efficient fluorophores with wide range of applications in biological labelling[1-3] and cell imaging, as logic gates and ion sensors,[4-6] and in dye-sensitized solar cells[7-10] and solution-processed bulk hyperconjunction solar cells.[11,12] BODIPYs exhibits excellent properties such as sharp absorption and fluorescence bands in the visible region, reasonably high fluorescence quantum yields, large molar absorption coefficients and are highly stable towards light and chemicals.[13-15] The properties of BODIPYs can be fine-tuned by introducing substituents at the pyrrole carbons, *meso* carbon as well as replacing fluorides present on the boron.[13-15] On the other hand, porphyrins are the most widely investigated tetrapyrrolic aromatic macrocycles because of their importance in biochemical processes[16-18] such as oxygen transfer and storage (hemoglobin and myoglobin), electron transfer (cytochrome c, cytochrome oxidase) and energy conversion (chlorophyll).[19-21] Because of large cavity and presence of four pyrrole nitrogens, porphyrins form a great number of complexes with metal ions[22-24] and some nonmetals.[25,26] The coordinating environment provided by porphyrins is very flexible and can be fine-tuned to particular oxidation and spin states by varying peripheral substitution and axial ligands.[25]

BODIPYs and porphyrins have complementary light absorbing properties. BODIPYs absorb strongly at ~500 nm whereas porphyrins absorb strongly in 420-450 nm region and moderately in 500-700 nm region.[27,28] Thus, the BODIPY-porphyrin conjugates resulted by linking BODIPY to porphyrin either covalently or noncovalently absorb over a broad range in the visible region which is highly desirable for enhancing the light-harvesting efficiency throughout the solar spectrum. In recent times, several elegant BODIPY-porphyrin conjugates in which BODIPY and porphyrin units are connected either covalently[29] or non-covalently[30] were

RSC Advances Accepted Manuscript

View Article Online
DOI: 10.1039/C4RA10807H

Published on 19 November 2014. Downloaded by University of Chicago on 19/11/2014 19:01:19.

synthesized and explored their energy/electron transfer properties. Some of these conjugates have also been incorporated into dye-sensitized semiconductor solar cells to improve light harvesting ability of the photo-electrochemical cells.[30] However, a perusal of literature revealed that porphyrins having boron-dipyrromethenyl unit as one of its *meso*-substituent is almost scarce although there are several reports on covalently linked BODIPY-porphyrin conjugates.[29] This is because of unavailability of proper precursors and appropriate synthetic strategies. Herein we report *meso*-boron dipyrromethenyl porphyrins **1-3** and mono-functionalized *meso*-boron dipyrromethenyl porphyrin building blocks **4-7** by condensing 2-formyl *meso*-anisyl BODIPY[31] **10** with *meso*-anisyl dipyrromethane **11** and desired substituted benzaldehyde under mild acid catalyzed conditions. To demonstrate the use of *meso*-BODIPYnyl porphyrin building blocks, we prepared *meso*-BODIPYnyl porphyrin-BF_2 smaragdyrin conjugate **8** and the preliminary photophysical studies indicated an efficient energy transfer from *meso*-BODIPYnyl porphyrin to BF_2 smaragdyrin unit.[32]

Results and Discussion

The required 2-formyl *meso*-anisyl BODIPY **10** was prepared by treating *meso*-anisyl BODIPY[27] with the Vilsmeier reagent in 1,2-dichloroethane at reflux temperature, followed by column chromatographic purification on silica as reported in literature. The other required precursor, *meso*-anisyl dipyrromethane **11** was prepared according to Lindsey's procedure[33] by condensing *p*-anisyl benzaldehyde with excess pyrrole in the presence of a catalytic amount of trifluoroacetic acid at room temperature followed by flash silica gel column chromatographic purification. The desired *meso*-BODIPYnyl porphyrins and functionalized *meso*-BODIPYnyl porphyrins **1-7** were prepared under mild acid catalyzed conditions by condensing one equivalent of 2-formyl *meso*-anisyl BODIPY[31] **10** with two equivalents of *meso*-anisyl dipyrromethane **11**

RSC Advances Accepted Manuscript

View Article Online
DOI: 10.1039/C4RA10807H

Published on 19 November 2014. Downloaded by University of Chicago on 19/11/2014 19:01:19.

and one equivalent of appropriate substituited/functionalized aryl aldehyde in the presence of catalytic amount of trifluoroacetic acid in CH_2Cl_2 at room temperature followed by oxidation with DDQ. The progress of the condensation reaction was followed by TLC analysis which showed one minor fast moving spot and one more polar major spot. The crude compounds were subjected to alumina column chromatographic purification and the fast moving *meso*-tetraryl porphyrins were removed and the desired *meso*-BODIPYnyl porphyrins **1-7** were collected in 5-7% yields. The compounds **1-7** were confirmed by HR-MS, detailed 1D, 2D, ^{13}C, ^{11}B and ^{19}F NMR techniques. The molecular structures of compounds **1-7** were deduced by detailed ^{1}H NMR, ^{1}H-^{1}H COSY and NOESY spectral studies as outlined below for compound **1**. The ^{1}H NMR spectrum along with key regions of ^{1}H-^{1}H COSY and NOESY spectra for compound **1** are shown in Fig. 1. The coupling constants in the ^{1}H NMR (Fig. 1a) spectrum and cross-peak connectivities in the ^{1}H-^{1}H COSY (Fig. 1b) and NOESY (Fig. 1c) spectra were used to identify all of the proton resonances. To assign all of these resonances, we picked out the -OCH_3 resonance of *meso*-anisyl group (*type I*) of BODIPY unit which appeared as singlet at 3.87 ppm corresponding to three protons. The *type I* methoxy protons showed NOE correlation with ortho protons (*type o*) of *meso*-anisyl group which appeared as doublet at 7.08 ppm. The *type o* resonance at 7.08 ppm showed cross peak correlation with a doublet at 7.82 which we identified as *type n* protons of *meso*-anisyl group of BODIPY unit of compound **1**. The *type n* resonance showed NOE correlation with a doublet at 7.18 ppm which we assigned to the *type a* pyrrole proton of BODIPY unit. The resonances at 6.70 ppm and 8.10 ppm were identified as *type b* and *type c* pyrrole protons of BODIPY unit of compound **1** based on their cross peak correlations in the COSY spectrum. The singlet at 7.74 ppm was ascribed to *type d* pyrrole proton as this resonance showed NOE correlation with *type n* resonance at 7.82 ppm. The other singlet

RSC Advances Accepted Manuscript

View Article Online
DOI: 10.1039/C4RA10807H

Published on 19 November 2014. Downloaded by University of Chicago on 19/11/2014 19:01:19.

resonance at 8.71 ppm was ascribed to *type e* pyrrole proton. Both *type d* and *type e* resonances showed NOE correlation with a doublet in most downfield region at 9.12 ppm which we identified as *type f* pyrrole protons of porphyrin unit of compound **1**. The doublet resonance at 8.90 ppm was assigned to *type g* pyrrole protons of porphyrin unit as this resonance showed cross-peak correlation with *type f* resonance at 9.12 ppm. The *meso*-anisyl protons of porphyrin unit (*type II*) which appeared as singlet at 4.10 ppm showed NOE correlation with a resonance at 7.28 ppm which we identified as *type m* protons of *meso*-anisyl group of porphyrin unit of compound **1**. The resonance at 8.10 ppm was identified as *type l* protons of *meso*-anisyl group of porphyrin unit based on its cross-peak correlation with a *type m* resonance at 7.28 ppm. The *type h* pyrrole resonance of porphyrin appeared at 8.84 ppm was identified as this resonance showed NOE correlation with *type l* resonance at 8.10 ppm. The resonance at 8.84 ppm was assigned to *type i* proton based on cross-peak correlation with *type h* resonance in COSY. The -CH_3 protons of *meso*-tolyl group (*type III*) of porphyrin unit appeared as singlet resonance at 2.70 ppm showed NOE correlation with resonance at 7.54 ppm which we identified as *type k* protons of *meso*-tolyl group of porphyrin unit of compound **1**. The *type k* protons showed cross-peak correlation with resonance at 8.10 ppm which we assigned to *type j* protons of *meso*-tolyl group of porphyrin. The inner NH proton of porphyrin was appeared as broad singlet at -2.72 ppm. Thus, all of the signals of compound **1** were assigned on the basis of ^{1}H-^{1}H COSY and NOESY NMR spectroscopic studies. The other compounds **2-7** also showed similar features and all protons were identified and assigned on similar basis. All compounds showed typical quartet at ~ -144 ppm in ^{19}F NMR and a triplet at 0.99 ppm in ^{11}B NMR with negligible shifts compared to *meso*-phenyl BODIPY.[34] We also prepared Zn(II) and Ni(II) derivatives of compound **1** by treating it with appropriate metal salt in $CHCl_3$ or CH_3OH at reflux conditions followed by

RSC Advances Accepted Manuscript

View Article Online
DOI: 10.1039/C4RA10807H

column chromatographic purifications to afford corresponding metal derivatives **Zn1** and **Ni1** in decent yields. The **Zn1** and **Ni1** were confirmed by mass spectrometry and ^{1}H, ^{11}B and ^{19}F NMR techniques.

Photophysical and electrochemical properties

The absorption properties of compounds **1**-**7** were studied in $CHCl_3$ and the data is summarized in Table 1. The comparison of absorption spectra of compound **1** with 5, 10, 15, 20-*meso*-tetra(*p*-tolyl)porphyrin (H_2TTP) is shown in Fig. 2a. As is clear from fig. 2 and data in Table 1 that compounds **1**-**7** showed four bands in 450-700 nm region and one Soret band at 420 nm. The presence of BODIPY unit at the *meso*-position of porphyrin unit significantly alters the electronic properties of the porphyrin and compounds **1**-**7** show three well defined Q-bands and one Soret band instead of four well-defined Q-bands observed for *meso*-tetrararylporphyrins such as H_2TTP. For example compound **1** showed absorption bands at 420, 490, 515, 597 and 663 nm. In these, the bands at 420, 515, 597 and 663 nm are mainly due to porphyrin ring whereas the band at 490 nm is due to BODIPY unit. Furthermore, the absorption bands of compounds **1-7** are generally broad with higher extinction coefficients and the Q_1 band showed ~20-25 nm bathochromic shift compared to H_2TTP. Thus, the presence of BODIPY unit at the *meso*-position alters the π-delocalization of the porphyrin macrocycle.

The redox properties of compounds **1**-**7** along with H_2TTP are probed through cyclic voltammetric studies using 0.1 M tetrabutylammonium perchlorate as supporting electrolyte (TBAP) in dichloromethane as solvent. The cyclic voltammogram of compound **1** is compared with H_2TTP in Fig. 2b and the data for all compounds **1**-**7** along with H_2TTP are tabulated in Table 2. As clear from the fig. 2b and data presented in Table 2 that all compounds **1**-**7** showed two quasi-reversible oxidations and three reversible/quasi-reversible reductions. For example,

Published on 19 November 2014. Downloaded by University of Chicago on 19/11/2014 19:01:19.

RSC Advances Accepted Manuscript

View Article Online
DOI: 10.1039/C4RA10807H

Published on 19 November 2014. Downloaded by University of Chicago on 19/11/2014 19:01:19.

compound **1** showed two oxidations at 1.06 and 1.23 V and three reductions at -0.59, -1.10 and -1.49 V. In these, the two oxidations at 1.23 and 1.06 V were exclusively due to porphyrin unit; the two reductions at -1.10 and -1.49 V were due to porphyrin ring whereas the reduction at -0.59 V was due to BODIPY unit. These assignments were made based on the data of their reference compounds, BODIPY[34] and H_2TTP.[28] Interestingly, the oxidation and reduction potentials of porphyrin in compounds **1-7** did not vary much compared to H_2TTP[28] except the presence of additional reduction wave corresponding to reduction of *meso*-BODIPY moiety. However, the compounds **1-7** are very stable under redox conditions. Furthermore, we realized that compounds **1-7** were completely non-fluorescent although both BODIPY and porphyrin units are decently fluorescent systems. In fact, it has been demonstrated earlier in several covalently linked BODIPY-porphyrin conjugates, the occurrence of efficient energy transfer from BODIPY unit to porphyrin unit on selective excitation of BODIPY unit.[35-38] The non-fluorescence behaviour of compounds **1-7** indicate that there is a possibility of electron transfer instead of energy transfer between BODIPY and porphyrin moieties in conjugates **1-7**. Furthermore, the strong excitonic interactions between the two moieties also perturb the energy levels leading to the enhancement of nonradiatve decay processes. However, the detailed studies are required to understand the excited state dynamics of these compounds.

The absorption spectra of **Zn1** and **Ni1** showed two Q-bands and one strong Soret band which were bathochromically shifted compared to ZnTTP and NiTTP respectively.[39] The electrochemical studies of **Zn1** and **Ni1** were carried out in CH_2Cl_2 using TBAP as supporting electrolyte and the data were included in Table 2 along with ZnTTP and NiTTP. It is clear from the data presented in Table 2 that both **Zn1** and **Ni1** showed one additional reduction at ~ -0.58 V corresponding to BODIPY moiety along with two oxidations and one or two reductions

RSC Advances Accepted Manuscript

View Article Online
DOI: 10.1039/C4RA10807H

Published on 19 November 2014. Downloaded by University of Chicago on 19/11/2014 19:01:19.

corresponding to metalloporphyrin unit. However, the metalloporphyrin centered oxidations and reductions of **Zn1** and **Ni1** were almost in the same potential range of those of ZnTTP and NiTTP[39] respectively.

Covalently linked *meso*-BODIPYnyl porphyrin-BF_2-smaragdyrin conjugate 8

To show the further use of functionalized *meso*-BODIPYnyl porphyrins, we synthesized one example of covalently linked *meso*-BODIPYnyl porphyrin-BF_2-smaragdyrin conjugate under mild Pd(0) coupling conditions as shown in Scheme 2. The reaction was carried out by coupling of compound **7** with ethynyl BF_2-smaragdyrin[32] **9** in the presence of catalytic amounts of $[Pd_2(dba)_3]$ and $AsPh_3$ at 35° C in toluene/triethylamine for 12 h. The progress of the reaction was followed by TLC analysis which showed the appearance of new spot corresponding to the desired compound and almost disappearance of spots corresponding to the starting precursors **7** and **9**. After standard work-up and silica gel column chromatographic purification afforded the desired compound **8** in 90% yield. The molecular ion peak in ES-MS spectrum confirmed the identity of the compound **8**. The comparison of ^{1}H NMR spectra of compound **8** along with its constituted building blocks **7** and **9** is shown in Fig. 3. In ^{1}H NMR of compound **8** (Fig. 3c), the resonances were assigned on the basis of the spectra observed for the corresponding building blocks **7** (Fig. 3b) and **9** (Fig. 3a). In ^{1}H NMR spectrum of **8** (Fig. 3c), the additional five sets of signals observed in the region of 9 to 10.4 ppm were due to eight pyrrole protons and two furan protons of smaragdyrin moiety. As clear from Fig. 3, the ^{1}H NMR of compound **8** was composed of a super imposition of the spectra of **7** and **9** with negligible shifts in their chemical shifts indicating that *meso*-BODIPYnyl-porphyrin and BF_2-smaragdyrin moieties in compound **8** interact weakly and retain most of their individual ^{1}H NMR spectral features. The compound **8** showed one triplet at 1.01 ppm and one broad resonance at -12.17 ppm in ^{11}B NMR

RSC Advances Accepted Manuscript

View Article Online
DOI: 10.1039/C4RA10807H

Published on 19 November 2014. Downloaded by University of Chicago on 19/11/2014 19:01:19.

corresponding to boron atom of BODIPY moiety and smaragdyrin macrocycle respectively. It has been shown earlier that the boron present in the smaragdyrin macrocycle[32] experiences strong macrocyclic ring current effect and appears as broad signal at high field region. Similar observations were made in ^{19}F NMR spectra recorded for compound **8** which showed a typical quartet at -144 ppm for BODIPY moiety and a broad resonance at -149 ppm corresponding to the BF_2-smaragdyrin macrocycle. The absorption, electrochemical and fluorescence properties of compound **8** (Fig. 4) along with its associated reference compounds were studied and the relevant data were included in Table 1. The comparison of absorption spectra of compound **8** along with its associated reference compounds **7** and **9** is shown in Fig. 4a. As clear from the fig. 4a, the absorption spectrum of **8** in both Q-band and Soret region showed the absorption features of both the moieties and the absorption spectrum of **8** was almost identical to that of the 1:1 mixture of monomers indicating that the two moieties interact weakly and retain their individual characteristic features. The cyclic voltammogram of compound **8** recorded in CH_2Cl_2 using tetrabutylammonium perchlorate as supporting electrolyte showed four reductions at -0.59, -0.89, -1.07 and -1.44 V and three oxidations at 0.79, 1.12 and 1.39 V (Fig. 4b). In this, the reduction at -0.59 V corresponding to BODIPY moiety; the oxidation at 0.79 V and reduction at -0.89 V were exclusively due to smaragdyrin moiety; oxidation at 1.12 V and reduction at -1.07 V were exclusively due to porphyrin moiety and the remaining oxidation at 1.30 V and reduction at -1.44 were due to both porphyrin and smaragdyrin moieties. Thus, the electrochemical study of compound **8** also showed features of BODIPY, porphyrin and smaragdyrin moieties with slight shifts in its potential compared to reference monomers.[28,32,34] This supports weak interaction among the BODIPY, porphyrin and smaragdyrin moieties in compound **8**. The fluorescence spectrum of compound **8** recorded at 510 nm where BODIPY unit absorbs exclusively showed

RSC Advances Accepted Manuscript

View Article Online
DOI: 10.1039/C4RA10807H

Published on 19 November 2014. Downloaded by University of Chicago on 19/11/2014 19:01:19.

emission band at 724 nm corresponding to smaragdyrin unit with a quantum yield of 0.016 indicating a possibility of intramolecular energy transfer from *meso*-BODIPYnyl porphyrin unit to smaragdyrin unit in compound **8**. However, The quantum yield of BF_2-smaragdyrin unit in compound **8** was quenched by 84% compared to free BF_2-smaragdyrin[32] (Φ = 0.10) indicating that the energy transfer is not the predominant process and there is a possibility of the photo-induced electron transfer between *meso*-BODIPYnyl porphyrin and BF_2-smaragdyrin units. Thus, our preliminary photophysical studies indicated the possibility of both photoinduced energy- and electron transfer processes, the detailed studies are required to probe excited state dynamics of compound **8** and *meso*-BODIPYnyl porphyrins **1-7**.

Conclusions

In conclusion, we prepared *meso*-BODIPYnyl porphyrin building blocks by condensing 2-formyl BODIPY with *meso*-anisyl dipyrromethane and functionalized aldehyde under mild acid catalyzed conditions. The presence of BODIPYnyl group directly at one of the *meso*-position alters the π-delocalization of the porphyrin macrocycle which reflected in their bathochromically shifted absorption bands and weak fluorescence behaviour. The electrochemical study indicated that *meso*-BODIPYnyl porphyrins are stable under redox conditions. The weak fluorescence of *meso*-BODIPYnyl porphyrins compared to *meso*-tetraaryl porphyrins indicates the possibility of electron transfer between BODIPY and porphyrin moieties in *meso*-BODIPYnyl porphyrins. The *meso*-BODIPYnyl porphyrin was connected covalently to BF_2-smaragdyrin unit covalently under Pd(0) coupling conditions and the resultant *meso*-BODIPYnyl porphyrin-BF_2-smaragdyrin conjugate showed features of both the *meso*-BODIPYnyl porphyrin and BF_2-smaragdyrin units as evidenced by spectral and electrochemical studies. The steady state fluorescence studies on *meso*-BODIPYnyl-BF_2-smaragdyrin conjugate

RSC Advances Accepted Manuscript

View Article Online
DOI: 10.1039/C4RA10807H

Published on 19 November 2014. Downloaded by University of Chicago on 19/11/2014 19:01:19.

also indicated that the photo-induced electron transfer is also possible along with energy transfer between *meso*-BODIPYnyl porphyrin and BF_2-smsragdyrin moieties. These types of *meso*-BODIPYnyl porphyrins and *meso*-BODIPYnyl porphyrin-BF_2-smaragdyrin conjugates have potential applications in molecular electronics and material science.

Experimental Section

General

The chemicals such as $BF_3{\cdot}OEt_2$, trifluoroacetic acid (TFA), and 2, 3-dichloro-5,6-dicyano-1,4-benzoquinone (DDQ) were used as obtained from Aldrich. All other chemicals used for the synthesis were reagent grade unless otherwise specified. Column chromatography was performed on silica (60-120 mesh) and basic alumina. The 1D, 2D, ^{13}C, ^{11}B and ^{19}F NMR spectra were recorded in $CDCl_3$ on Bruker 400 and 500 MHz instrument. The frequency for ^{13}C nucleus is 100 MHz, 470.54 MHz for ^{19}F nucleus, and 160.46 MHz for ^{11}B nucleus. Tetramethylsilane [$Si(CH_3)_4$] was used as an internal standard for ^{1}H and ^{13}C NMR, tetrafluorotoluene as a external standard for ^{19}F NMR and boric acid as an external standard for ^{11}B NMR. Absorption and steady state fluorescence spectra were obtained with Varian. The fluorescence quantum yields (Φ) were estimated from the emission and absorption spectra by comparative method at the excitation wavelength of 420 nm using H_2TTP (Φ = 0.11) as standard.[40] Cyclic voltammetric (CV) studies were carried out with BAS electrochemical system utilizing the three electrode configuration consisting of a glassy carbon (working electrode), platinum wire (auxiliary electrode) and saturated calomel (reference electrode) electrodes. The experiments were done in dry dichloromethane using 0.1 M tetrabutylammonium perchlorate as supporting electrolyte. The high resolution mass spectra (HRMS) were recorded with a Bruker maxis Impact and Q-Tof micro mass spectrometer. For UV-vis and fluorescence titrations, the

RSC Advances Accepted Manuscript

View Article Online
DOI: 10.1039/C4RA10807H

Published on 19 November 2014. Downloaded by University of Chicago on 19/11/2014 19:01:19.

stock solution of all compounds (5×10^{-6} and 2.5×10^{-6} M) were prepared by using HPLC grade $CHCl_3$ solvent.

General procedure for the synthesis of compounds 1-7

Samples of *β*-formyl *meso*-anisyl BODIPY **10**[31] (100 mg, 0.306 mmol), dipyrromethane **11**[33] (154 mg, 0.613 mmol) and aldhyde **12** (0.306 mmol) in 50 mL CH_2Cl_2 were stirred in presence of 30 μL TFA under nitrogen for 2 h. DDQ was added and the stirring was continued in air for an additional 1.5 h. The reaction mixture was neutralized with triethylamine and the solvent was removed on rotary evaporator. The crude product was purified by basic alumina column chromatography using petroleum ether/dichloromethane (60:40, v/v) and afforded pure compound (**1-7**) as a purple solid.

Compound 1: 7% Yield (20 mg), ^{1}H NMR (500 MHz, $CDCl_3$, δ in ppm): -2.72 (s, 2H; NH), 2.70 (s, 3H; -CH_3), 3.87 (s, 3H; OCH_3), 4.10 (s, 6H; -OCH_3), 6.70 (dd, ^3J (H, H) = 4.2, 4.1 Hz, 1H; Py), 7.08 (d, ^3J (H, H) = 8.7 Hz, 2H; Ar), 7.18 (d, ^3J (H, H) = 4.1 Hz, 1H; Py), 7.28 (q, ^3J (H, H) = 8.6 Hz, 4H; Ar), 7.54 (q, ^3J (H, H) = 7.8 Hz, 2H; Ar), 7.74 (s, 1H; py), 7.82 (d, ^3J (H, H) = 8.5 Hz, 2H; Ar), 8.08-8.13 (m, 7H; Ar, Py), 8.71 (s, 1H; Py), 8.84-8.85 (m, 4H; py), 8.90 (d, ^3J (H, H) = 4.5 Hz, 2H; Py), 9.12 (d, ^3J (H, H) = 4.6 Hz, 2H; Py). ^{11}B NMR (160.4 MHz, $CDCl_3$, δ in ppm): 0.99 (t, ^1J (B-F) = 28 Hz, B). ^{19}F NMR (470.5 MHz, $CDCl_3$, δ in ppm): -144.6 (q, ^1J (F-B) = 28 Hz, F). ^{13}C NMR (100 MHz, $CDCl_3$, δ in ppm): 55.7, 55.8, 112.4, 114.5, 118.8, 120.2, 120.4, 120.5, 120.7, 120.8, 126.6, 127.7, 132.0, 132.9, 134.2, 134.6, 134.7, 134.8, 134.9, 135.8, 135.9, 137.7, 139.3, 144.2, 146.6, 148.8, 159.7, 162.5. UV-vis (in $CHCl_3$, λ_{max}/nm, logε) = 420 (5.5), 490 (4.8), 515 (4.8), 597 (4.3), 663 (4.2). HRMS. Calcd for $C_{57}H_{44}BF_2N_6O_3$ [$(M+H)^+$]: m/z 909.3540. Found: m/z 909.3541.

RSC Advances Accepted Manuscript

View Article Online
DOI: 10.1039/C4RA10807H

Published on 19 November 2014. Downloaded by University of Chicago on 19/11/2014 19:01:19.

Compound 2: 6% Yield (20 mg), ^{1}H NMR (500 MHz, $CDCl_3$, δ in ppm): -2.72 (s, 2H; NH), 3.86 (s, 3H; OCH_3), 4.10 (s, 9H; -OCH_3), 6.70 (dd, ^{3}J (H, H) = 4.3, 4.2 Hz, 1H; Py), 7.08 (d, ^{3}J (H, H) = 8.9 Hz, 2H; Ar), 7.17 (d, ^{3}J (H, H) = 4.0 Hz, 1H; Py), 7.28-7.31 (m, 6H; Ar), 7.75 (s, 1H; py), 7.83 (d, ^{3}J (H, H) = 8.9 Hz, 2H; Ar), 8.10-8.13 (m, 7H; Ar, Py), 8.71 (s, 1H; Py), 8.84-8.85 (m, 4H; py), 8.90 (d, ^{3}J (H, H) = 4.5 Hz, 2H; Py), 9.12 (d, ^{3}J (H, H) = 4.6 Hz, 2H; Py). ^{11}B NMR (160.4 MHz, $CDCl_3$, δ in ppm): 0.98 (t, ^{1}J (B-F) = 28 Hz, B). ^{19}F NMR (470.5 MHz, $CDCl_3$, δ in ppm): -144.6 (q, ^{1}J (F-B) = 28 Hz, F). ^{13}C NMR (100 MHz, $CDCl_3$, δ in ppm): 53.6, 55.69, 55.7, 55.8, 110.9, 112.4, 114.5, 118.9, 120.3, 120.4, 126.5, 120.7, 132.0, 132.9, 134.2, 134.6, 134.7, 135.8, 135.9, 144.2, 146.6, 148.8, 159.7, 159.7, 162.5. UV-vis (in $CHCl_3$, λ_{max}/nm, logε) = 421 (5.5), 491 (4.8), 510 (4.8), 598 (4.3), 663 (4.1). HRMS. Calcd for $C_{57}H_{44}BF_2N_6O_4$ [$(M+H)^+$]: m/z 925.3489. Found: m/z 925.3429.

Compound 3: 5 % Yield (15 mg), ^{1}H NMR (400 MHz, $CDCl_3$, δ in ppm): -2.72 (s, 2H; NH), 3.86 (s, 3H; OCH_3), 4.10 (s, 6H; -OCH_3), 6.70 (dd, ^{3}J (H, H) = 4.2, 4.1 Hz, 1H; Py), 7.08 (d, ^{3}J (H, H) = 8.4 Hz, 2H; Ar), 7.17 (d, ^{3}J (H, H) = 4.2 Hz, 1H; Py), 7.27-7.30 (m, 4H; Ar), 7.74-7.78 (m, 4H; Ar, py), 7.83 (d, ^{3}J (H, H) = 7.8 Hz, 2H; Ar), 8.10-8.13 (m, 5H; Ar, Py), 8.20 (d, ^{3}J (H, H) = 7.7 Hz, 2H; Ar), 8.71 (s, 1H; Py), 8.82 (d, ^{3}J (H, H) = 4.6 Hz, 2H; py), 8.86 (d, ^{3}J (H, H) = 4.5 Hz, 2H; Py), 8.90 (d, ^{3}J (H, H) = 4.7 Hz, 2H; Py), 9.12 (d, ^{3}J (H, H) = 4.6 Hz, 2H; Py). ^{11}B NMR (160.4 MHz, $CDCl_3$, δ in ppm): 0.99 (t, ^{1}J (B-F) = 28 Hz, B). ^{19}F NMR (470.5 MHz, $CDCl_3$, δ in ppm): -144.6 (q, ^{1}J (F-B) = 28 Hz, F). ^{13}C NMR (100 MHz, $CDCl_3$, δ in ppm): 55.7, 55.8, 112.4, 114.5, 120.4, 120.4, 125.9,126.9, 128.0, 132.9, 134.8, 135.8, 135.9, 144.3, 159.7, 162.5. UV-vis (in $CHCl_3$, λ_{max}/nm, logε) = 420 (5.3), 491 (4.6), 509 (4.5), 596 (4.1), 662 (4.0). HRMS. Calcd for $C_{56}H_{42}BF_2N_6O_4$ [$(M+H)^+$]: m/z 895.3383. Found: m/z 895.3329.

RSC Advances Accepted Manuscript

View Article Online
DOI: 10.1039/C4RA10807H

Published on 19 November 2014. Downloaded by University of Chicago on 19/11/2014 19:01:19.

Compound 4: 6% Yield (17 mg), ^{1}H NMR (500 MHz, $CDCl_3$, δ in ppm): -2.71 (s, 2H; NH), 3.86 (s, 3H; OCH_3), 4.09 (s, 6H; -OCH_3), 6.71 (dd, ^{3}J (H, H) = 4.2, 4.1 Hz, 1H; Py), 7.09 (d, ^{3}J (H, H) = 8.8 Hz, 2H; Ar), 7.18 (d, ^{3}J (H, H) = 4.2 Hz, 1H; Py), 7.27-7.30 (m, 4H; Ar), 7.75 (s, 1H; py), 7.82 (d, ^{3}J (H, H) = 8.7 Hz, 2H; Ar), 8.05-8.09 (m, 2H; Ar), 8.10-8.12 (m, 5H; Ar, py), 8.31-8.33 (m, 2H; Ar), 8.69 (d, ^{3}J (H, H) = 4.4 Hz, 2H; py), 8.85 (s, 1H; Py), 8.89-8.92 (m, 4H; py), 9.14 (d, ^{3}J (H, H) = 4.3 Hz, 2H; Py). ^{11}B NMR (160.4 MHz, $CDCl_3$, δ in ppm): 0.99 (t, ^{1}J (B-F) = 28 Hz, B). ^{19}F NMR (470.5 MHz, $CDCl_3$, δ in ppm): -144.6 (q, ^{1}J (F-B) = 28 Hz, F). ^{13}C NMR (100 MHz, $CDCl_3$, δ in ppm): 55.7, 55.8, 55.8 112.4, 112.5, 114.5, 117.5, 119.2, 120.4, 120.8, 126.6, 130.8, 132.2, 134.2, 134.4, 135.1, 135.2, 135.9, 144.6, 146.4, 147.4 148.9, 159.7, 159.8, 162.5. UV-vis (in $CHCl_3$, λ_{max}/nm, logε) = 421 (5.4), 4.90 (4.7), 510 (4.6), 597 (4.3), 662 (4.1). HRMS. Calcd for $C_{57}H_{41}BF_2N_7O_3$ [$(M+H)^+$]: m/z 920.3336. Found: m/z 920.3337.

Compound 5: 7 % Yield (19 mg), ^{1}H NMR (500 MHz, $CDCl_3$, δ in ppm): -2.72 (s, 2H; NH), 3.86 (s, 3H; OCH_3), 4.10 (s, 6H; -OCH_3), 6.72 (dd, ^{3}J (H, H) = 4.3, 4.2 Hz, 1H; Py), 7.08 (d, ^{3}J (H, H) = 8.9 Hz, 2H; Ar), 7.18 (d, ^{3}J (H, H) = 4.3 Hz, 1H; Py), 7.29-7.31 (m, 4H; Ar), 7.75 (s, 1H; py), 7.82 (d, ^{3}J (H, H) = 8.9 Hz, 2H; Ar), 8.10-8.12 (m, 5H; Ar, py), 8.37-8.40 (m, 2H; Ar), 8.62-8.62-8.65 (m, 2H; Ar), 8.70 (d, ^{3}J (H, H) = 4.9 Hz, 2H; py), 8.85 (s, 1H; Py), 8.90-8.92 (m, 4H; py), 9.14 (d, ^{3}J (H, H) = 4.5 Hz, 2H; Py). ^{11}B NMR (160.4 MHz, $CDCl_3$, δ in ppm): 0.99 (t, ^{1}J (B-F) = 28 Hz, B). ^{19}F NMR (470.5 MHz, $CDCl_3$, δ in ppm): -144.6 (q, ^{1}J (F-B) = 28 Hz, F). ^{13}C NMR (100 MHz, $CDCl_3$, δ in ppm): 55.7, 55.8, 112.2, 112.4, 112.5, 114.6, 116.9, 119.2, 120.9, 122.1, 125.9, 126.6, 128.1, 132.3, 132.9, 134.2, 134.4, 134.7, 135.3, 135.9, 144.6, 146.4, 147.9, 148.9, 149.4, 159.7, 162.5. UV-vis (in $CHCl_3$, λ_{max}/nm, logε) = 421 (5.3), 489 (4.7), 511 (4.7), 595 (4.3), 662 (4.1). HRMS. Calcd for $C_{56}H_{41}BF_2N_7O_5$ [$(M+H)^+$]: m/z 940.3234. Found: m/z 940.3233.

RSC Advances Accepted Manuscript

View Article Online
DOI: 10.1039/C4RA10807H

Published on 19 November 2014. Downloaded by University of Chicago on 19/11/2014 19:01:19.

Compound 6: 7% Yield (21 mg), ^{1}H NMR (400 MHz, $CDCl_3$, δ in ppm): -2.75 (s, 2H; NH), 3.86 (s, 3H; OCH_3), 4.10 (s, 6H; -OCH_3), 6.71 (dd, ^{3}J (H, H) = 4.2, 4.1 Hz, 1H; Py), 7.08 (d, ^{3}J (H, H) = 8.8 Hz, 2H; Ar), 7.18 (d, ^{3}J (H, H) = 4.0 Hz, 1H; Py), 7.28-7.31 (m, 4H; Ar), 7.75 (s, 1H; py), 7.82 (d, ^{3}J (H, H) = 8.9 Hz, 2H; Ar), 7.84-7.90 (m, 2H; Ar), 8.06-8.09 (m, 2H; Ar), 8.10-8.12 (m, 5H; Ar, py), 8.70 (s, 1H; py), 8.79 (d, ^{3}J (H, H) = 4.6 Hz, 2H; Py), 8.85-8.86 (m, 2H; py), 8.87 (d, ^{3}J (H, H) = 4.7 Hz, 2H; Py), 9.12 (d, ^{3}J (H, H) = 4.4 Hz, 2H; Py). ^{11}B NMR (160.4 MHz, $CDCl_3$, δ in ppm): 0.99 (t, ^{1}J (B-F) = 28 Hz, B). ^{19}F NMR (470.5 MHz, $CDCl_3$, δ in ppm): -144.6 (q, ^{1}J (F-B) = 28 Hz, F). ^{13}C NMR (100 MHz, $CDCl_3$, δ in ppm): 55.7, 55.9, 112.4, 114.5, 120.5, 130.1, 132.9, 135.7, 135.8, 136.0, 136.1, 144.4, 148.8, 159.7, 162.5. UV-vis (in $CHCl_3$, λ_{max}/nm, logε) = 420 (5.4), 490 (4.7), 510 (4.7), 595 (4.3), 662 (4.1). HRMS. Calcd for $C_{56}H_{41}BBrF_2N_6O_3$ [$(M+H)^+$]: m/z 973.2488. Found: m/z 973.2493.

Compound 7: 6% Yield (20 mg), ^{1}H NMR (500 MHz, $CDCl_3$, δ in ppm): -2.72 (s, 2H; NH), 3.86 (s, 3H; OCH_3), 4.10 (s, 6H; -OCH_3), 6.72 (dd, ^{3}J (H, H) = 4.2, 4.1 Hz, 1H; Py), 7.08 (d, ^{3}J (H, H) = 8.9 Hz, 2H; Ar), 7.18 (d, ^{3}J (H, H) = 4.3 Hz, 1H; Py), 7.28-7.30 (m, 4H; Ar), 7.74 (s, 1H; py), 7.82 (d, ^{3}J (H, H) = 8.8 Hz, 2H; Ar), 7.92-7.95 (m, 2H; Ar), 8.08-8.12 (m, 7H; Ar, py), 8.70 (s, 1H; Py), 8.79 (d, ^{3}J (H, H) = 4.6 Hz, 2H; py), 8.87 (d, ^{3}J (H, H) = 4.8 Hz, 2H; Py), 8.90 (d, ^{3}J (H, H) = 4.5 Hz, 2H; Py), 9.12 (d, ^{3}J (H, H) = 4.4 Hz, 2H; Py). ^{11}B NMR (160.4 MHz, $CDCl_3$, δ in ppm): 0.99 (t, ^{1}J (B-F) = 28 Hz, B). ^{19}F NMR (470.5 MHz, $CDCl_3$, δ in ppm): -144.6 (q, ^{1}J (F-B) = 28 Hz, F). UV-vis (in $CHCl_3$, λ_{max}/nm, logε) = 421 (5.3), 491 (4.7), 507 (4.6), 595 (4.3), 662 (4.1). HRMS. Calcd for $C_{56}H_{41}BF_2IN_6O_3$ [$(M+H)^+$]: m/z 1021.2350. Found: m/z 1021.2349.

Zn1 and Ni1 complexes:

RSC Advances Accepted Manuscript

View Article Online
DOI: 10.1039/C4RA10807H

Published on 19 November 2014. Downloaded by University of Chicago on 19/11/2014 19:01:19.

A solution of compound **1** (10 mg, 0.011 mmol) and an excess of $Zn(OAc)_2$/$Ni(OAc)_2$ in dichloromethane/methanol (3:1, 30 mL) was refluxed for 4 h. The crude compound was purified by basic alumina column chromatography using petroleum ether/dichloromethane (50:40, v/v) to afford pure compound **Zn1/ Ni1** as a purple solids.

Compound Zn1: 60% Yield (7mg), ^{1}H NMR (500 MHz, $CDCl_3$, δ in ppm): 2.71 (s, 3H; -CH_3), 3.83 (s, 3H; OCH_3), 4.10 (s, 6H; -OCH_3), 6.70 (dd, ^3J (H, H) = 4.2, 4.1 Hz, 1H; Py), 7.04 (d, ^3J (H, H) = 8.6 Hz, 2H; Ar), 7.15 (d, ^3J (H, H) = 4.2 Hz, 1H; Py), 7.28 (q, ^3J (H, H) = 8.6 Hz, 4H; Ar), 7.54-7.56 (m, 2H; Ar), 7.73 (s, 1H; py), 7.82 (d, ^3J (H, H) = 8.2 Hz, 2H; Ar), 8.07-8.12 (m, 7H; Ar, Py), 8.71 (s, 1H; Py), 8.95-8.96 (m, 4H; py), 8.99-9.01 (m, 2H; Py), 9.21-9.23 (m, 2H; Py). ^{11}B NMR (160.4 MHz, $CDCl_3$, δ in ppm): 0.99 (t, ^1J (B-F) = 28 Hz, B). ^{19}F NMR (470.5 MHz, $CDCl_3$, δ in ppm): -144.6 (q, ^1J (F-B) = 28 Hz, F). UV-vis (in $CHCl_3$, λ_{max}/nm, logε) = 423 (5.4), 494 (4.6), 557 (4.4), 662 (4.1). HRMS. Calcd for $C_{57}H_{42}BF_2N_6O_3Zn$ [$(M+H)^+$]: m/z 971.2671. Found: m/z 971.2679.

Compound Ni1: 70% Yield (7 mg), ^{1}H NMR (400 MHz, $CDCl_3$, δ in ppm): 2.64 (s, 3H; -CH_3), 3.86 (s, 3H; OCH_3), 4.05 (s, 6H; -OCH_3), 6.68 (dd, ^3J (H, H) = 4.3, 4.2 Hz, 1H; Py), 7.04 (d, ^3J (H, H) = 8.7 Hz, 2H; Ar), 7.14 (d, ^3J (H, H) = 4.0 Hz, 1H; Py), 7.19-7.22 (m, 4H; Ar), 7.48-7.50 (m, 2H; Ar), 7.54 (s, 1H; py), 7.75 (d, ^3J (H, H) = 8.7 Hz, 2H; Ar), 7.87-7.92 (m, 6H; Ar, Py), 8.08 (s, 1H; Py), 8.53 (s, 1H; Py), 8.74-8.78 (m, 4H; py), 8.79-8.80 (m, 2H; Py), 8.98-9.01 (m, 2H; Py). ^{11}B NMR (160.4 MHz, $CDCl_3$, δ in ppm): 0.99 (t, ^1J (B-F) = 28 Hz, B). ^{19}F NMR (470.5 MHz, $CDCl_3$, δ in ppm): -144.6 (q, ^1J (F-B) = 28 Hz, F). UV-vis (in $CHCl_3$, λ_{max}/nm, logε) = 417 (5.1), 487 (4.5), 514 (4.4), 538 (4.5), 594 (4.1).

Covalently linked *meso*-BODIPYnyl porphyrin-BF_2-smaragdyrin conjugate 8

RSC Advances Accepted Manuscript

View Article Online
DOI: 10.1039/C4RA10807H

Published on 19 November 2014. Downloaded by University of Chicago on 19/11/2014 19:01:19.

Compound **7** (10 mg, 0.0098 mmol) and 5, 10-(4-methyl-phenyl)-19-(4-ethynylphenyl)-25-oxasmaragdyrin **9**[34] (7 mg, 0.0098 mmol) were dissolved in dry toluene/Et_3N (6 ml, 5:1) in a 25 ml, two necked round-bottomed flask fitted with a reflux condenser, gas inlet and outlet tubes for nitrogen purging. The reaction mixture was placed in an oil bath preheated to 35 °C. After purging the flask with nitrogen for 15 min, $AsPh_3$ (3.5 mg, 0.0117 mmol) and $Pd_2(dba)_3$ (1.5 mg, 0.0014 mmol) were added, and the reaction mixture was stirred at 35 °C for 12 h. TLC analysis of the reaction mixture indicated the appearance of a dark new spot apart from the two minor spots corresponding to the unreacted starting precursor. The solvent was removed under reduced pressure and the crude compound was purified by basic alumina column chromatography. The excess $AsPh_3$ and the small amount of unreacted starting precursors were removed with petroleum ether and the required pure compound **8** was then collected with petroleum ether/CH_2Cl_2. 90% Yield (13 mg), ^{1}H NMR (500 MHz, $CDCl_3$, δ in ppm): -3.79- 3.81 (m, 2H; NH), -2.69 (s, 2H; NH), 2.81 (s, 6H; CH_3), 3.90 (s, 3H; -OCH_3), 4.10 (s, 6H; -OCH_3), 6.71-6.73 (m, 1H; Py), 7.08-7.11 (m, 2H; Ar), 7.18-7.20 (m, 1H; Py), 7.03-7.34 (m, 4H; Ar), 7.60 (d, ^3J (H, H) = 7.60 Hz, 4H; Ar), 7.74 (d, ^3J (H, H) = 7.7 Hz, 1H; Py), 7.83-7.86 (m, 2H; Ar), 8.12-8.17 (m, 7H; Ar, Py), 8.28-8.33 (m, 8H; Ar), 8.70 (d, ^3J (H, H) = 7.6 Hz, 2H; Ar), 8.74 (s, 1H; Py), 8.89-8.94 (m, 4H; Py), 8.98 (d, ^3J (H, H) = 4.7 Hz, 2H; Py), 9.01-9.02 (m, 2H; Py), 9.15 (d, ^3J (H, H) = 4.5 Hz, 2H; Py), 9.49 (s, 2H; Oxa), 9.66 (d, ^3J (H, H) = 4.3 Hz, 2H; Py), 10.24-10.25 (m, 2H; Py), 10.35 (d, ^3J (H, H) = 4.4 Hz, 2H; Py). ^{11}B NMR (160.4 MHz, $CDCl_3$, δ in ppm): 1.01 (t, ^1J (B-F) = 27 Hz, 1B), -12.17 (s, B). ^{19}F NMR (470.5 MHz, $CDCl_3$, δ in ppm): -144.6 (q, ^1J (F-B) = 28 Hz, F), -149.3 (s, 2F). UV-vis (in $CHCl_3$, λ_{max}/nm, logε) = 422 (5.4), 451 (5.5), 477 (4.9), 593 (4.9), 633 (4.4), 654 (4.5), 709 (4.8). LRMS Calcd for $C_{101}H_{71}B_2F_4IN_{10}O_4$ [$(M+H)^+$]: m/z 1584.5322. Found: m/z 1585.5561.

RSC Advances Accepted Manuscript

View Article Online
DOI: 10.1039/C4RA10807H

Acknowledgements

We thank the Department of Science and Technology, Government of India for financial support and S. K thanks the UGC for a fellowship.

Published on 19 November 2014. Downloaded by University of Chicago on 19/11/2014 19:01:19.

References

1. S. Kolemen, Y. Cakmak, Z. Kostereli and E. Akkaya, *Org. Lett*., 2014, **16**, 660.

2. F. Marsico, A. Turshatov, K. Weber and F. R. Wurm, *Org. Lett*., 2013, **15**, 3844.

3. A. B. Nepomnyashchii and A. J. Bard, *Acc. Chem. Res.*, 2012, **45**, 1844.

4. K. Umezawa, D. Citterio and K. Suzuki, *Analytical Sciences,* 2014, **30**, 327.

5. X. Qu, Q. Liu, X. Ji, H. Chen, Z. Zhou and Z. Shen, *Chem. Commun.,* 2012, **48**, 4600.

6. N. Bones, V. Leen and W. Dehaen, *Chem. Soc. Rev.,* 2012, **41**, 1130.

7. S. P. Singh and T. Gayathri, *Eur. J. Org. Chem.*, 2014, **22**, 4689.

8. H.-Y. Lin, W.-C. Huang, Y.-C. Chen, H.-H. Chou, C.-Y. Hsu, J. T. Lin and H.-W. Lin, *Chem. Commun.,* 2012, **48**, 8913.

9. R. Guliyev, S. Qzturk, E. Sahin and E. U. Akkaya, *Org. Lett.,* 2012, **6**, 1528.

10. J.-F. Lefebvre, X.-Z. Sun, J. A. Calladine, M. W. George and E. A. Gibson, *Chem. Commun*., 2014, **50**, 5258.

11. N. Boens, V. Leen, W. Dehaen, L. Wang, K. Robeyns, W. Qin, X. Tang, D. Beljonne, C. Tonnelé, J. M. Paredes, M. J. R.-Rama, A. Orte, L. Crovetto, E. M. Talavera and M. A.-Pez, *J. Phys. Chem*., 2012, **116**, 9621.

12. A. Mirloup, N. Leclerc, S. Rihn, T. Bura, R. Bechara, A. Hébraud, P. Lévêque, T. Hiser and R. Ziessel, *New J. Chem*., 2014, **38**, 3644.

13. G. Ulrich, R. Ziessel and A. Harriman, *Angew. Chem. Int. Ed.*, 2008, **47**, 1184.

RSC Advances Accepted Manuscript

View Article Online
DOI: 10.1039/C4RA10807H

Published on 19 November 2014. Downloaded by University of Chicago on 19/11/2014 19:01:19.

14. A. Loudet and K. Burgess, *Chem. Rev.*, 2007, **107**, 4891.

15. R. Ziessel, G. Ulrich and A. Harriman, *New J. Chem.,* 2007, **31**, 496.

16. G. Kodis, P. A. Liddell, L. de la Garza, P. C. Clausen, J. S. Lindsey, A. L. Moore, T.A. Moore and D. Gust, *J. Phys. Chem*. *A.,* 2002, **106**, 2036.

17. A. K. Burrell, D. L. Officer, P. G. Plieger and D. C. W. Reid, *Chem. Rev.,* 2001, **101**, 2751.

18. Y. Nakamura, I. W. Hwang, N. Aratani, T. K. Ahn, D. M. Ko, A. Takagi, T. Kawai, T. Matsumoto, D. Kim and A. Osuka, *J. Am. Chem. Soc.,* 2005, **127**, 236.

19. B. E. Murphy, S. A. Krasnikov, N. N. Sergeeva, A. A. Cafolla, A. B. Preobrajenski, A. N. Chaika, O. Lubben and I. V. Shvets, *Acs. Nano.,* 2014, **8**, 5190.

20. D. Kiessling, R. D. Costa, G. Katsukis, J. Malig, F. Lodermeyer, S. Feihl, A. Roth, L. Wibmer, M. Kehrer, M. Volland, P. Wagner, G. G. Wallace, D. I. Officer and D. M. Guldi, *Chem. Sci*., 2013, **4**, 3085.

21. H. J. Son, S. Jin, S. Patwardhan, S. J. Wezenberg, N. C. Jeong, M. So, C. E. Wilmer, A. A. Sarjeant, G. C. Schatz, R. Q. Snurr, O. K. Farha, G. P. Wiederrecht and J. T. Hupp, *J. Am*. *Chem. Soc*., 2013, **135**, 862.

22. M. Zhang, Z.-Y. Gu, M. Bosch, Z. Perry and H.-C. Zhou, *Coord, Chem. Rev*., 2014, http://dx.doi.org/10.1016/j.ccr.2014.05.031.

23. R. A. Baglia, M. Dürr, I. I. Burmazović and D. P. Goldberg, *Inorg. Chem*., 2014, **53**, 5893.

24. L. Pan, X. Huang, H. –L. N. Phan, T. J. Emge, J. Li and X. Wang, *Inorg. Chem*., 2004, **43**, 6878.

25. P. D. Harvey, K. M. Kadish, K. M. Smith and R. Guilard, *The Porphyrin Handbook*, 2003.

26. L. Giribabu, T. A. Rao and B. G. Maiya, *Inorg. Chem*., 1999, **38**, 4971.

RSC Advances Accepted Manuscript

View Article Online
DOI: 10.1039/C4RA10807H

Published on 19 November 2014. Downloaded by University of Chicago on 19/11/2014 19:01:19.

27. H. L. Kee, C. Kirmaier, L. Yu, P. Thamyongkit, W. J. Youngblood, M. E. Calder, L. Ramos, B. C. Noll, D. F. Bocain, W. R. Scheidt, R. R. Birge, J. S. Lindsey and D. Holten, *J. Phys. Chem. B.*, 2005, **109**, 20433.

28. D. Kim and A. Osuka, *Acc. Chem. Res*., 2004, **37**, 735.

29. C. Jiao, L. Zhu and J. Wu, *Chem, Eur, J.,* 2011, **17**, 6610.

30. T. K. Khan, M. Broring, S. Mathur and M. Ravikanth, *Coord. Chem. Rev*., 2013, **257**, 2348.

31. L. Jiao, C. Yu, J. Li, Z. Wang, M. Wu and E. Hao, *J. Org. Chem.,*2009, **74**, 7525.

32. M. R. Rao and M. Ravikanth, *J. Org. Chem*., 2011, **76**, 3582.

33. B. J. Littler, M. A. Miller, C.–H. Hung, R. W. Wagner, D. F. O'Shea, P. D. Boyle and J. S. Lindsey, *J. Org. Chem.,*1999, **64**, 7890.

34. V. Lakshmi and M. Ravikanth, *Dalton Trans*., 2012, **41**, 5903.

35. R. W. Wagner, J. S. Lindsey, J. Seth, V. Palaniappan and D. F. Bocian, *J. Am. Chem. Soc.,* 1996, **118**, 3996.

36. F. Li, S. I. Yang, Y. Ciringh, J. Seth, C. H. Martin, D. L. Singh, D. Kim, R. R. Birge, D. F. Bocian, D. Holten and J. S. Lindsey, *J. Am. Chem. Soc.,* 1998, **120**, 10001.

37. T. K. Khan and M. Ravikanth, *Tetrahedron*., 2011, **67**, 5816.

38. J.–Y. Liu, E. A. Ermilov, B. RÖder and D. K. P. Ng, *J. porphyrins phthalocyanines*., 2013, **17**, 831.

39. J. Wojaczynski and L. L.-Grażyński, *Coord. Chem. Rev*., 2000, **204**, 113.

40. G. Santosh and M. Ravikanth, *Tetrahedron*., 2007, **63**, 7833.

RSC Advances Accepted Manuscript

View Article Online
DOI: 10.1039/C4RA10807H

Published on 19 November 2014. Downloaded by University of Chicago on 19/11/2014 19:01:19.

Legends

Scheme 1: Synthesis of compounds **1-7**.

Scheme 2: Synthesis of compound **8**.

Table 1: Absorption data of H_2TTP, **Zn1**, **Ni1** and compounds **1-10** recorded in $CHCl_3$. Concentration of solution used for soret band is $2.5x10^{-6}$ and for Q band is $5x10^{-6}$ M.

Table 2: Electrochemical (V) data of BODIPY, H_2TTP, ZnTTP, NiTTP, **Zn1**, **Ni1** and compounds **1-9** recorded in CH_2Cl_2 containing 0.1 M TBAP as the supporting electrolyte recorded at 50 mVs^{-1} scan speed.

Fig. 1: (a) ^1H NMR, (b) ^1H-^1H COSY and (c) NOESY spectrum of compound **1** recorded in $CDCl_3$.

Fig. 2: (a) Comparison of normalized absorption of H_2TTP (red line) and compound **1** black line) recorded in $CHCl_3$. The inset shows the expansion of soret bands. The concentration used for Q-band spectra was $5x10^{-6}$ M and soret band spectrum was $2.5x10^{-6}$ M. (b) Comparison of cyclic voltammogram of BODIPY (i), H_2TTP (ii) and compound **1** (iii) recorded in CH_2Cl_2.

Fig. 3: Comparison of ^1H NMR spectra of (a) Ethynyl BF_2-smaragdyrin **9,** (b) compound **7** and (c) compound **8**.

Fig. 4: (a) Comparison of normalized absorption of compound **7** (black line), compound **9** (red line) and compound **8** (blue line) recorded in $CHCl_3$. The inset shows the expansion of soret bands. The concentration used for Q-band spectra was $5x10^{-6}$ M and soret band spectrum was $2.5x10^{-6}$. (b) Comparison of cyclic voltammogram of compound **9** (i), **7** (ii) and compound **8** (iii) recorded in CH_2Cl_2.

RSC Advances Accepted Manuscript

View Article Online
DOI: 10.1039/C4RA10807H

Published on 19 November 2014. Downloaded by University of Chicago on 19/11/2014 19:01:19.

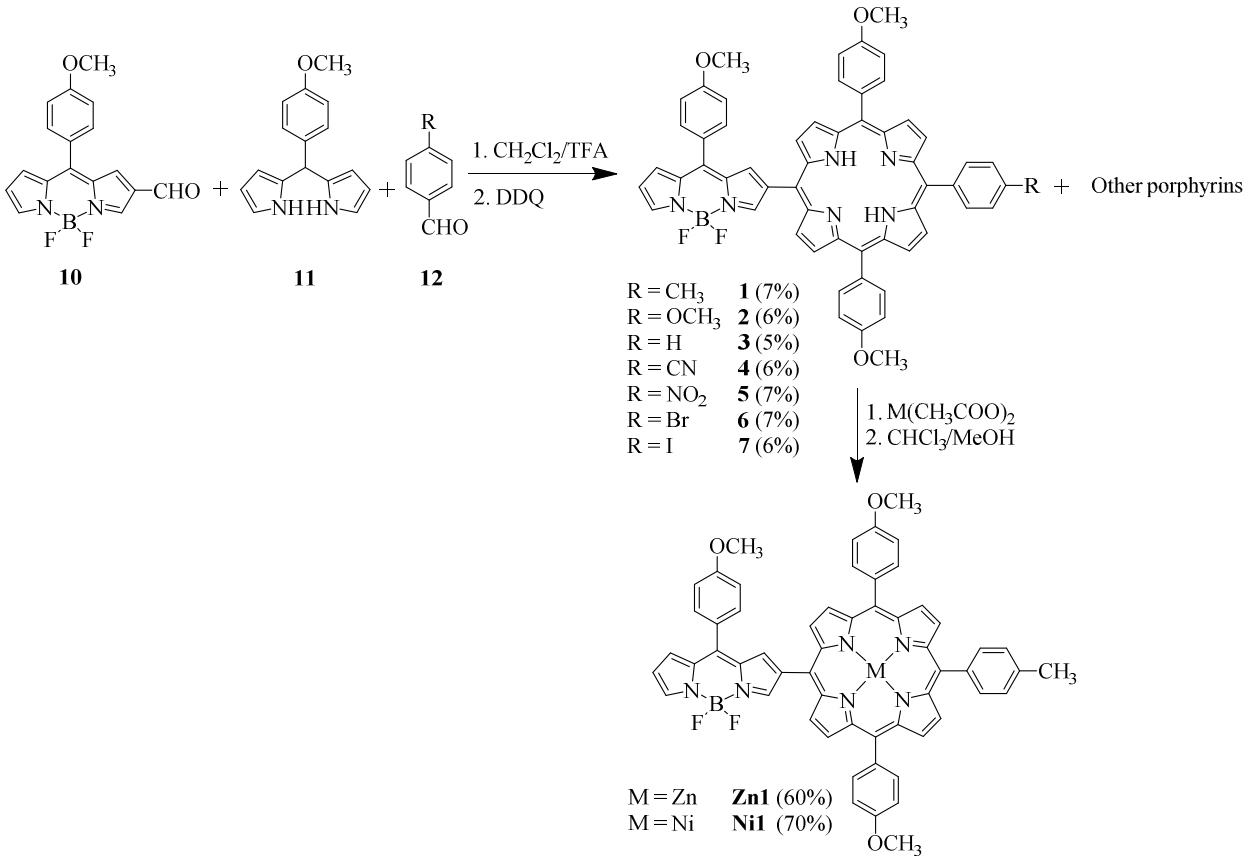

Scheme 1

RSC Advances Accepted Manuscript

View Article Online
DOI: 10.1039/C4RA10807H

Published on 19 November 2014. Downloaded by University of Chicago on 19/11/2014 19:01:19.

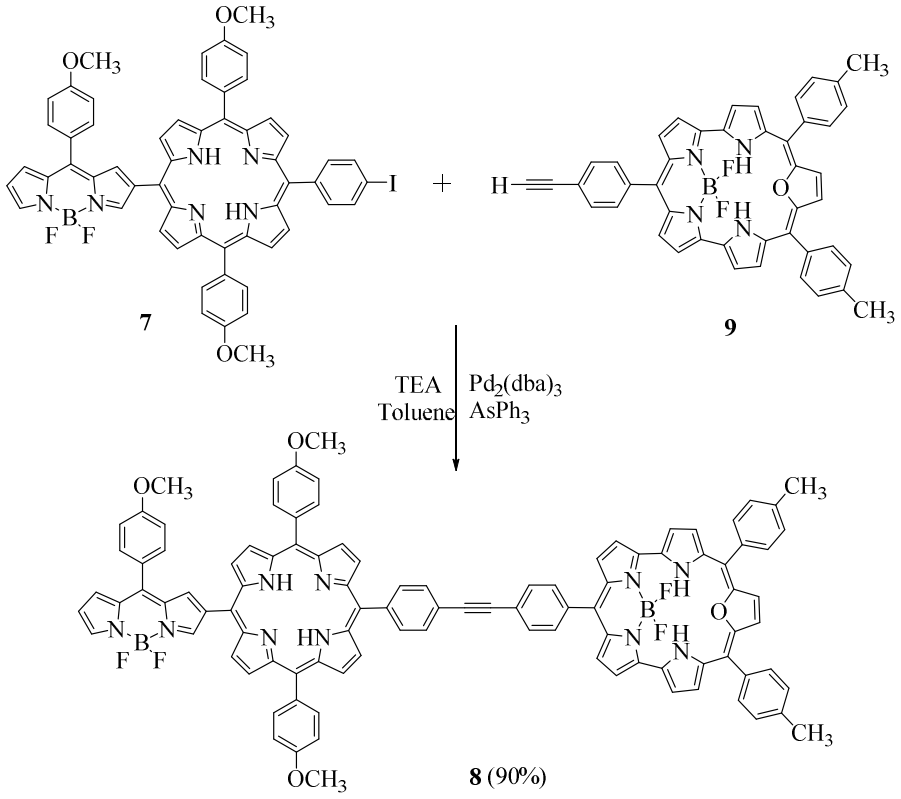

Scheme 2

RSC Advances Accepted Manuscript

View Article Online
DOI: 10.1039/C4RA10807H

Published on 19 November 2014. Downloaded by University of Chicago on 19/11/2014 19:01:19.

Table 1

Compound	Soret band (nm) (logε) ($mol^{-1}dm^3\ cm^{-1}$)	Q bands (nm) (logε) ($mol^{-1}dm^3\ cm^{-1}$)
H_2TTP	420(5.5)	517(4.1), 552(3.8), 591(3.5), 648(3.6)
1	420(5.5)	490(4.8), 515(4.8), 597(4.3), 663(4.2)
Zn1	423(5.4)	494(4.6), 557(4.4), 662(4.1)
Ni1	417(5.1)	487(4.5), 514(4.4), 538(4.5), 594(4.1)
2	421(5.5)	491(4.8), 510(4.8), 598(4.3), 663(4.1)
3	420(5.3)	491(4.6), 509(4.5), 596(4.1), 662(4.0)
4	421(5.4)	490(4.7), 510(4.6), 597(4.3), 662(4.1)
5	421(5.3)	489(4.7), 511(4.7), 595(4.3), 662(4.1)
6	420(5.4)	490(4.7), 510(4.7), 595(4.3), 662(4.1)
7	420(5.4)	491(4.7), 507(4.6), 595(4.3), 662(4.1)
8	422(5.43), 451(5.5),477(4.9)	512(4.7), 593(4.9), 633(4.4), 654(4.5), 709(4.8)
9	448(5.5), 476(5.1)	594(4.0), 632(4.2), 652(4.3), 707(4.6)
10	-	494(5.0)

RSC Advances Accepted Manuscript

View Article Online
DOI: 10.1039/C4RA10807H

Published on 19 November 2014. Downloaded by University of Chicago on 19/11/2014 19:01:19.

Table 2

Compound	$E_{1/2ox}$ (V/SCE)				$E_{1/2red}$ (V/SCE)		
	$E_{1/2sma}$	$E_{1/2por}$	$E_{1/2por/sma}$	$E_{1/2BDP}$	$E_{1/2sma}$	$E_{1/2por}$	$E_{1/2por/sma}$
BODIPY	-	-	-	-0.81	-	-	-
H_2TTP	-	1.12	1.35	-	-	-1.07	-1.40
ZnTTP	-	0.90	1.21	-	-	-1.17	-1.39
NiTTP	-	1.18	1.29	-	-	-1.14	-
9	0.78	-	1.22	-	-0.90	-	-1.42
1	-	1.06	1.23	-0.59	-	-1.10	-1.49
Zn1	-	0.89	1.18	-0.58	-	-1.22	-1.51
Ni1	-	1.16	1.28	-0.57	-	-1.18	-
2	-	1.05	1.20	-0.62	-	-1.13	-1.53
3	-	1.12	1.26	-0.62	-	-1.12	-1.55
4	-	1.15	1.29	-0.60	-	-1.07	-1.48
5	-	1.15	1.27	-0.60	-	-0.89	-1.51
6	-	1.12	1.26	-0.61	-	-1.12	-
7	-	1.13	1.27	-0.59	-	-1.08	-1.46
8	0.79	1.12	1.30	-0.59	-0.89	-1.07	-1.44

BDP = BODIPY, sma = smaragdyrin, por = porphyrin

RSC Advances Accepted Manuscript

View Article Online
DOI: 10.1039/C4RA10807H

Published on 19 November 2014. Downloaded by University of Chicago on 19/11/2014 19:01:19.

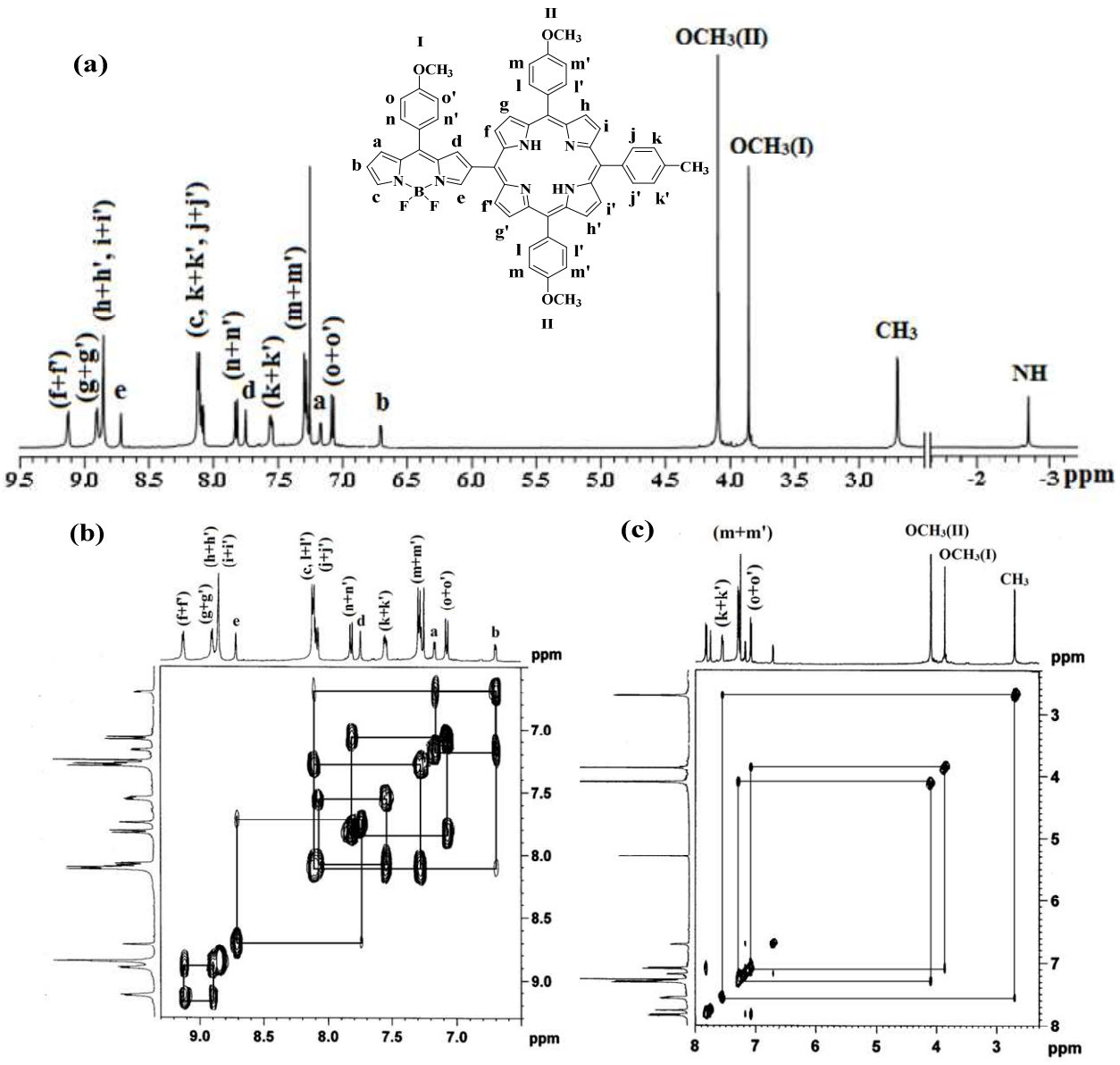

Fig. 1

RSC Advances Accepted Manuscript

View Article Online
DOI: 10.1039/C4RA10807H

Published on 19 November 2014. Downloaded by University of Chicago on 19/11/2014 19:01:19.

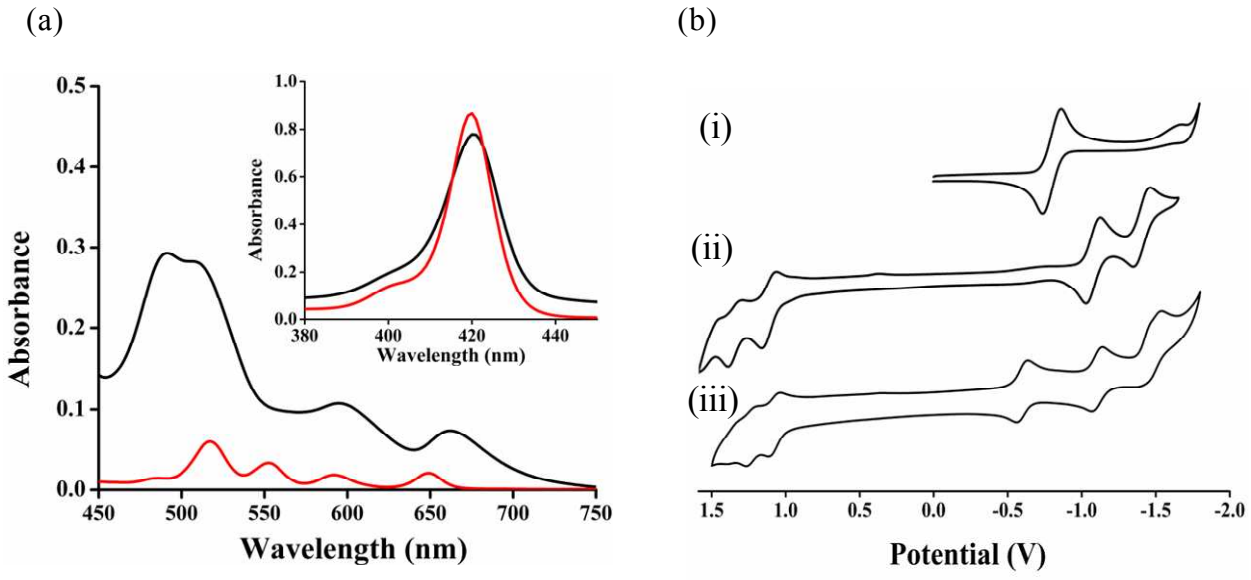

Fig. 2

RSC Advances Accepted Manuscript

View Article Online
DOI: 10.1039/C4RA10807H

Published on 19 November 2014. Downloaded by University of Chicago on 19/11/2014 19:01:19.

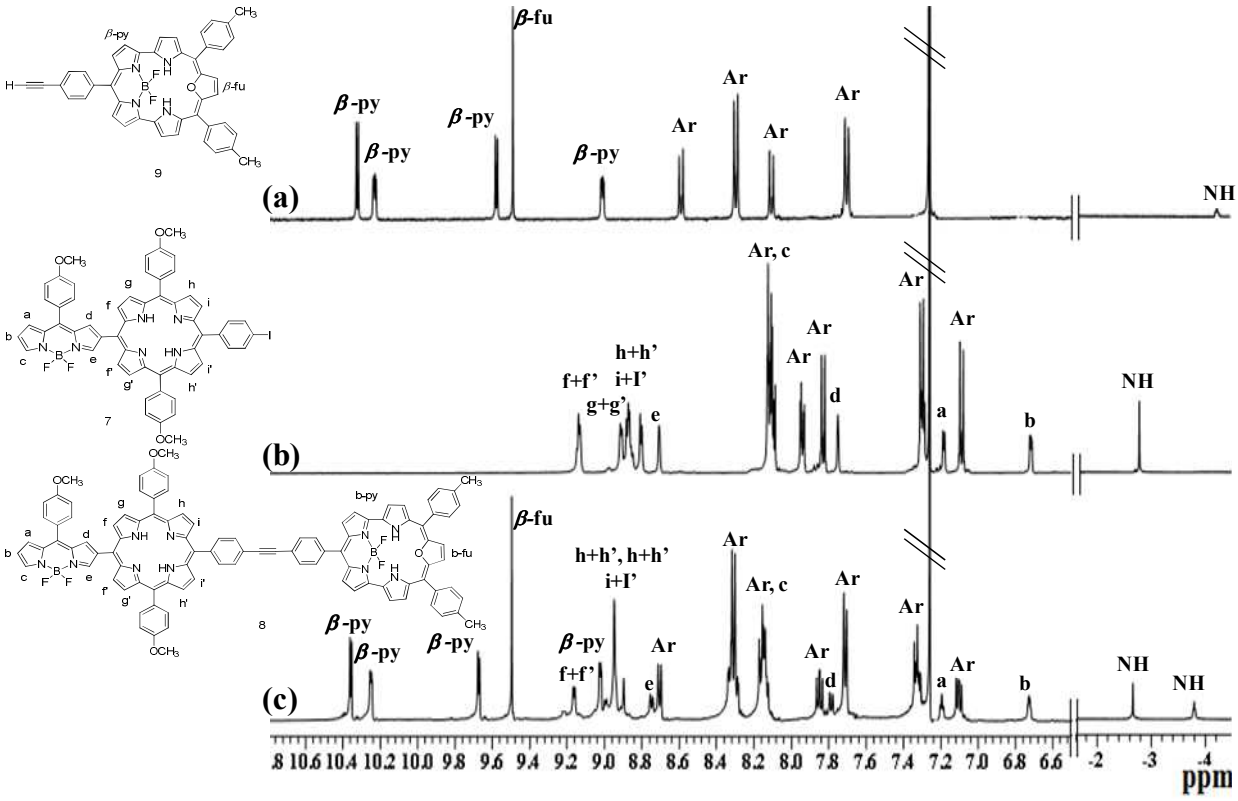

Fig. 3

RSC Advances Accepted Manuscript

View Article Online
DOI: 10.1039/C4RA10807H

Published on 19 November 2014. Downloaded by University of Chicago on 19/11/2014 19:01:19.

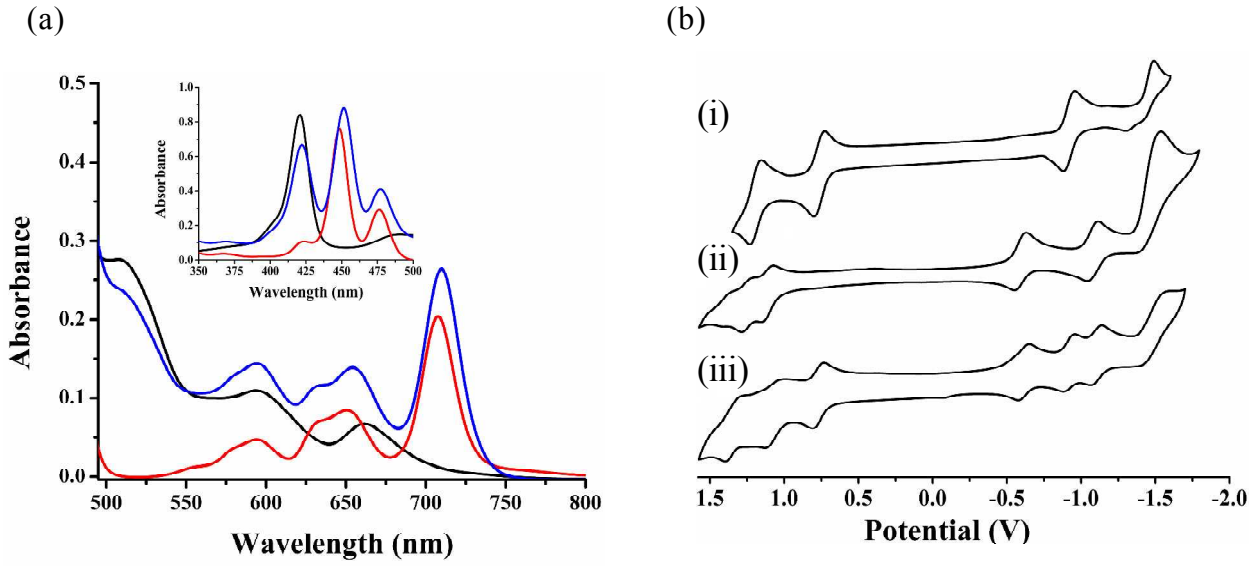

Fig. 4

RSC Advances Accepted Manuscript

View Article Online
DOI: 10.1039/C4RA10807H

Published on 19 November 2014. Downloaded by University of Chicago on 19/11/2014 19:01:19.

Graphical Abstract

2-Formyl Boron-Dipyrromethene as Key Synthon to Prepare Functionalized *Meso*-Boron Dipyrromethenyl Porphyrin Building Blocks

Sunit Kumar and Mangalampalli Ravikanth*

Indian Institute of Technology, Powai, Mumbai, 400076 India. Fax: 91-22-5723480

Tel: 91-22-5767176; E-mail: ravikanth@chem.iitb.ac.in

A series of functionalized *meso*-BODIPYnyl porphyrin building blocks were synthesized using 2-formyl BODIPY as key precursor.

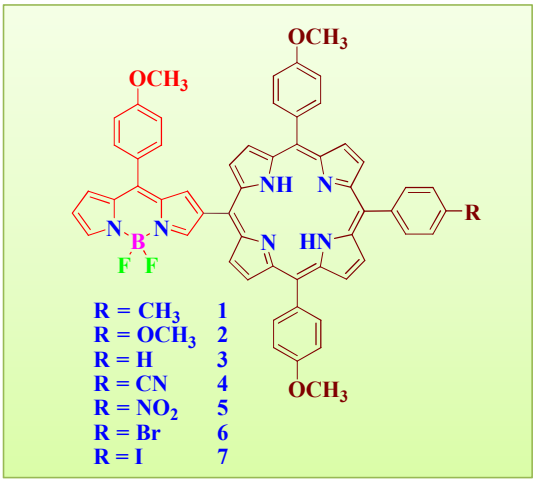

RSC Advances Accepted Manuscript